The full Low-carbon Expansion Generation Optimization (LEGO) model

S. Wogrin[a,b,*], D. Tejada-Arango[c,d], U. Bachhiesl[a], B.F. Hobbs[e]

[a] *Institute of Electricity Economics and Energy Innovation (IEE), Graz University of Technology, Graz, Austria*
[b] *Institute for Research in Technology (IIT), School of Engineering (ICAI), Comillas Pontifical University, Madrid, Spain*
[c] *Energy Management Consulting, AFRY, Madrid, Spain*
[d] *Facultad de Ciencias Económicas y Empresariales (ICADE), Universidad Pontificia Comillas, Madrid, Spain*
[e] *Department of Environmental and Health Engineering,Johns Hopkins University, Baltimore, USA*

Abstract

This paper introduces the full Low-carbon Expansion Generation Optimization (LEGO) model available on Github[1]. LEGO is a mixed integer quadratically constrained optimization problem and has been designed to be a multi-purpose tool, like a Swiss army knife, that can be employed to study many different aspects of the energy sector. Ranging from short-term unit commitment to long-term generation and transmission expansion planning. The underlying modeling philosophies are: modularity and flexibility. Its unique temporal structure allows LEGO to function with either chronological hourly data, or all kinds of representative periods. LEGO is also composed of thematic modules that can be added or removed from the model easily via data options depending on the scope of the study. Those modules include: unit commitment constraints; DC- or AC-OPF formulations; battery degradation; rate of change of frequency inertia constraints; demand-side management; or the hydrogen sector. LEGO also provides a plethora of model outputs (both primal and dual), which is the basis for both technical but also economic analyses. To our knowledge there is

*Corresponding author:
URL: wogrin@tugraz.at (S. Wogrin)
[1] https://github.com/wogrin/LEGO

no model that combines all of these capabilities, which we hereby make freely available to the scientific community.

Keywords: generation expansion planning, github, transmission expansion, open-source, optimization, power system

1. Introduction

To mitigate climate change, we as a society have embarked on the journey towards net-zero energy systems [1, 2]. Ahead of us there lie massive regulatory, social, economic and technical challenges such as the effective coupling of the electric power, heat and gas sectors, as well as the electrification of transport, active demand-side management and many more. Transparent, open-source energy system models (ESMs) are necessary to support the energy transition through more informed and better decision making. For an overview of non-open-source ESMs the reader is referred to [3].

In this paper, we want to introduce a newly developed open-source ESM called Low-carbon Expansion Optimization (LEGO) model. The LEGO model is a mixed-integer quadratically[2] constrained optimization problem (MIQCP) coded in GAMS [4]. The data is read directly from Excel and the results are also written to the same Excel file. LEGO has been designed to be a multi-purpose tool, like a Swiss army knife, that can be employed to study many different aspects of the energy sector. The underlying modeling philosophies are: modularity and flexibility. LEGO also provides a plethora of model outputs (both primal and dual).

LEGO is *modular* in the sense that it can be assembled with different thematic blocks that allow for a wide variety of specific analyses. These modules currently include: considering unit commitment (UC) decisions[3]; considering

[2]It is only quadratic if the SCOP formulation of the AC-OPF is solved, otherwise the model is a mixed-integer linear program (MILP).

[3]This module can be relaxed by solving LEGO as a relaxed Mixed Integer Program (rMIP).

(or not[4]) an electricity network; considering the electricity grid via a DC or an AC optimal power flow (OPF)[5] formulation; considering degradation for battery energy storage systems (BESS) via cycle aging costs; considering rate of change of frequency (RoCoF) system inertia constraints; considering demand-side management (DSM) via load shifting and load shedding; considering the hydrogen sector.

LEGO's model *flexibility* is currently three-fold: flexibility of running LEGO as a mixed integer program (MIP) and consider discrete decisions (such as lumpy investments and UC) or as a relaxed-MIP, where discrete variables are relaxed; flexibility of running an operation only or an investment (GEP, TEP or GEPTEP)[6] model; flexibility in the representation of time (representative periods, hourly models, time segments/blocks).

Let us now compare LEGO to some other available open-source ESMs. The GenX[7] model [5] originally developed at MIT is a powerful electricity resource capacity expansion planning tool. Some differences with respect to LEGO are the fact that GenX does not account for RoCoF constraints, and currently considers a zonal flow. A DC power flow is in development but there is not the option of considering an AC power flow. With respect to temporal flexibility, GenX works for chronological time periods (including representative days). LEGO can be run for both chronological and non-chronological time periods, and is capable of establishing inter-temporal constraints [6] between non-chronological representative periods, which allows to combine short- and long-term storage in aggregated optimization models. There are not many aggregated models that incorporate long-term storage as pointed out in [7]. The Electricity Market Model EMMA[8] [8] is a techno-economic dispatch and in-

[4]In this case, LEGO is converted into a single-node problem.

[5]In particular, we consider a second-order cone programming (SOCP) approximation of the full AC-OPF.

[6]We consider candidate investments in both generation expansion planning (GEP) and transmission expansion planning (TEP)

[7]https://github.com/GenXProject/GenX

[8]https://neon.energy/en/emma/

vestment model developed by NEON consulting company. EMMA does not account for hydro reservoir modeling, does not include DSM, RoCoF nor UC constraints, nor does it allow for discrete investment decisions. It also does not model an optimal power flow or the hydrogen sector. The openTEPES[9] model [9] developed at the Institute for Research in Technology of Comillas Pontifical University is a cost minimization GEPTEP model. Its time representation allows for chronological periods (of one or multiple hours); however, it does not allow for representation of non-chronological representative periods in combination with long-term storage technologies as LEGO does, nor does it consider an AC-OPF, RoCoF, DSM nor the hydrogen sector. The Next Energy Modeling system for Optimization (NEMO)[10] is an open-source energy system optimization tool developed by the Stockholm Environment Institute. NEMO does not allow for AC-OPF, nor does it consider RoCoF, DSM or hydrogen. The temporal structure uses (hierarchical) time slices, which need to be ordered in order to account for storage. The ANTARES[11] tool for adequacy reporting of electric systems [10], is an open source power system simulator to quantify the adequacy or the economic performance of interconnected energy systems. The underlying optimization models of ANTARES work with chronological time periods (hours within weeks). In order to incorporate long-term storage technologies, such as hydro, additional information, such as the current weekly water value, has to be incorporated as data. The temporal structure of LEGO is more flexible than that and does therefor not rely on exogenous data. Moreover, ANTARES does not incorporate DSM, the hydrogen sector nor an AC-OPF formulation.

DSM is gaining attention and importance in power systems, especially with respect to the integration of variable renewable energy sources [11] or otherwise improving system efficiency [12]. In LEGO, we wanted to include two types of DSM: one that was simple load shedding at a previously established cost; and

[9] https://github.com/IIT-EnergySystemModels/openTEPES
[10] https://github.com/sei-international/NemoMod.jl
[11] https://github.com/AntaresSimulatorTeam/Antares_Simulator

another, that was load shifting in order to be able to accommodate potentials of DSM via heating and cooling, electric vehicles (EVs) etc. There are several approaches in the literature to address shifting DSM. For example, [13] presents a DSM formulation that allows for load shifting but does not guarantee to avoid simultaneous up and downward shifting. In [14], the authors propose an alternative version of [13] that tries to circumvent this problem, but in order to do so, they have to introduce a downward DSM variable that depends on the temporal index twice. This means that the total number of downward DSM variables is the cardinality of the time index squared. An approach like this works when assessing one single representative day of 24 consecutive hourly time periods, but not when assessing long-term problems, where 8760 consecutive hours are analyzed. Based on [14], our DSM variables only depend on the time index, once, and we avoid simultaneous up and downward DSM by introducing binary variables.

With respect to hydrogen, currently, only few GEPTEP models consider hydrogen technologies and even less are open-source. As an example, the authors in [15] model a hydrogen technology chain formed by electrolyzer – methanization – storage tanks – OCGT – CCUS with symmetric charging and discharging capacity. However, their model is formulated as an LP which is not capable of considering discrete investment decisions. The comprehensive model presented in [5] considers a combination of electroyzer – hydrogen storage – fuel cell with asymmetric charging and discharging capacity but they only apply a simple transport problem to model inter-zonal power flows. Authors in [16] take a game-theoretic approach to modeling integrated planning of power and natural gas systems in a cooperative environment. They incorporate Power-to-Gas units with the option of providing up and downward reserve capacity. However, their model is formulated as an MINLP which is highly non-convex and non-linear. The authors in [17] propose a multi-objective model. They minimize the average costs of carbon emission reduction and maximize profits of Power-to-Gas units in order to determine their optimal capacity and grid connection points. Although their model focuses on transformation of integrated power and gas

systems they do not explicitly consider battery technologies.

LEGO is based on preliminary work [18] by the authors, and has been extended to incorporate many novel aspects, such as transmission expansion planning in both a DC- and AC framework, the introduction of DSM, the hydrogen sector, battery degradation, the economic output based on dual variables, and the fact that it is now freely available on Github[12]. To the best of our knowledge, there is no single open-source model available that combines all of the previously mentioned characteristics, which makes LEGO uniquely versatile.

The remainder of this paper is organized as follows. Section 2 discusses some further details about LEGO's modularity and flexibility options, as well as the model outputs. Section 3 contains the mathematical formulation of the LEGO model. In section 4, we present several case studies to showcase LEGO's modularity and flexibility. Finally, section 5 concludes the paper.

2. Modularity, flexibility and outputs of LEGO model

This section contains further details about how to utilize LEGO's modularity and flexibility via data, and finally discusses some of LEGO's data output.

2.1. Modularity

In the introduction, we have already discussed the different thematic modeling blocks[13] that LEGO offers. Each of these modules can be combined freely with the others, and it is as simple as activating a (yes/no) option in the data file in Excel. In the LEGO data file, there is a sheet named Parameters, shown in Figure 1, where these options can be chosen. For example, one can carry out a DC-OPF and study the impact on the production of hydrogen when allowing DSM.

[12] https://github.com/wogrin/LEGO

[13] UC, DC/AC-OPF, RoCoF, battery degradation, the hydrogen sector, DSM, etc.

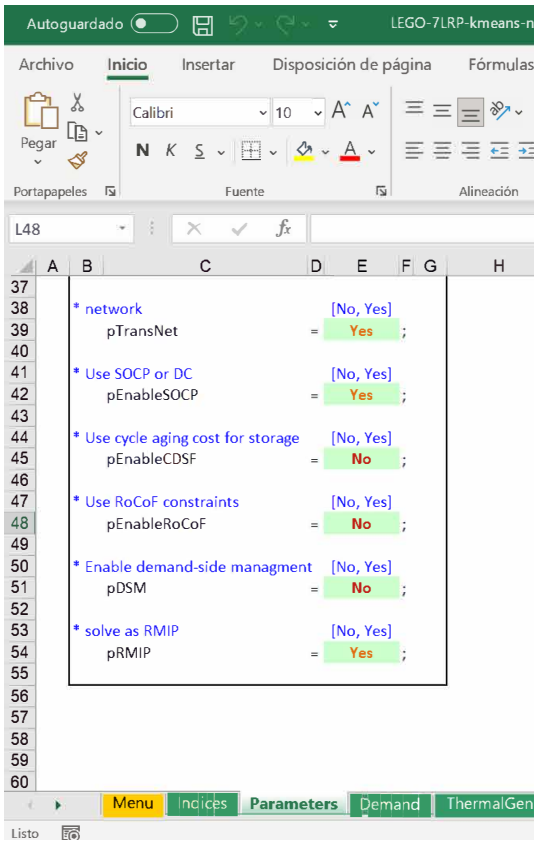

Figure 1: LEGO parameter sheet with model options.

2.2. Flexibility

Model flexibility, just like LEGO's modularity, can be tapped into easily via the data. This means that LEGO users do not have to bother to change the code or the model itself. They can simply access all of LEGO's flexibility via data input. Let us briefly describe how this can be achieved.

LEGO has been designed as a Mixed Integer Problem (MIP); the integrality stems from planning variables (i.e., investments) and operational (i.e., unit commitment, UC) decisions. Relaxing integrality on these two sets of variables renders a relaxed-MIP (rMIP) framework that still has physical meaning. This can be obtained using the *pRMIP* option shown in Figure 1.

With respect to running LEGO as an operation only or an investment model,

in the corresponding data sheet as seen in Figure 2, candidate transmission lines can be explicitly specified. If there are none, LEGO does not consider TEP. As for GEP, in LEGO one can specify how many of the units are existing (via parameter *ExisUnits*), whether or not generation expansion is possible for this type of unit (via parameter *EnableInvest*), and what is the maximum amount of this type of unit that can be built (via parameter *MaxInvest*), all of which can be seen in Figure 3.

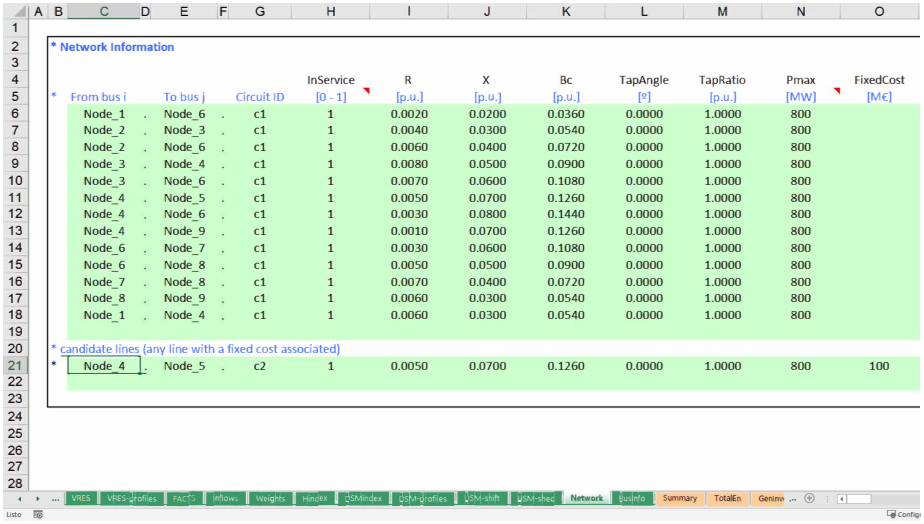

* Network information

* From bus i	To bus j	Circuit ID	InService [0 - 1]	R [p.u.]	X [p.u.]	Bc [p.u.]	TapAngle [º]	TapRatio [p.u.]	Pmax [MW]	FixedCost [M€]
Node_1	Node_6	c1	1	0.0020	0.0200	0.0360	0.0000	1.0000	800	
Node_2	Node_3	c1	1	0.0040	0.0300	0.0540	0.0000	1.0000	800	
Node_2	Node_6	c1	1	0.0060	0.0400	0.0720	0.0000	1.0000	800	
Node_3	Node_4	c1	1	0.0080	0.0500	0.0900	0.0000	1.0000	800	
Node_3	Node_6	c1	1	0.0070	0.0600	0.1080	0.0000	1.0000	800	
Node_4	Node_5	c1	1	0.0050	0.0700	0.1260	0.0000	1.0000	800	
Node_4	Node_6	c1	1	0.0030	0.0800	0.1440	0.0000	1.0000	800	
Node_4	Node_9	c1	1	0.0010	0.0700	0.1260	0.0000	1.0000	800	
Node_6	Node_7	c1	1	0.0030	0.0600	0.1080	0.0000	1.0000	800	
Node_6	Node_8	c1	1	0.0050	0.0500	0.0900	0.0000	1.0000	800	
Node_7	Node_8	c1	1	0.0070	0.0400	0.0720	0.0000	1.0000	800	
Node_8	Node_9	c1	1	0.0060	0.0300	0.0540	0.0000	1.0000	800	
Node_1	Node_4	c1	1	0.0060	0.0300	0.0540	0.0000	1.0000	800	
* candidate lines (any line with a fixed cost associated)										
* Node_4	Node_5	c2	1	0.0050	0.0700	0.1260	0.0000	1.0000	800	100

Figure 2: LEGO power network data including existing and candidate lines.

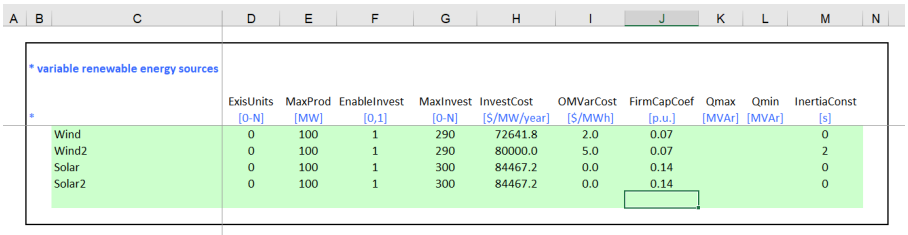

* variable renewable energy sources

*	ExisUnits [0-N]	MaxProd [MW]	EnableInvest [0,1]	MaxInvest [0-N]	InvestCost [$/MW/year]	OMVarCost [$/MWh]	FirmCapCoef [p.u.]	Qmax [MVAr]	Qmin [MVAr]	InertiaConst [s]
Wind	0	100	1	290	72641.8	2.0	0.07			0
Wind2	0	100	1	290	80000.0	5.0	0.07			2
Solar	0	100	1	300	84467.2	0.0	0.14			0
Solar2	0	100	1	300	84467.2	0.0	0.14			0

Figure 3: LEGO variable renewable energy sources data.

Let us now discuss in detail the type of temporal flexibility that LEGO allows for. In many energy modeling applications, such as running a UC model

for example, the desired temporal representation are chronological hours. Especially in applications studying the short term. Medium, or long-term models, however, might resort to representative periods (days or weeks), or even time slices [19] or load periods [20] to represent very long time horizons that would lead to computationally intractable models if chronological hourly periods were to be considered. Depending on the data input, LEGO allows for all these types of studies without having to adapt the model code and formulation, simply via the data.

In order to achieve this, we define three different temporal indices: p, k, rp, which are specified in the data sheet Indices, as seen in Figure 4, and which we will use throughout the model formulation. Index p represents the actual chronological periods (which are usually hourly but could even have a shorter duration); rp are the representative periods used; and finally, index k corresponds to the chronological periods within the representative period rp. In order for those indices, and corresponding variables, to have proper meaning, we also introduce weight parameters W_{rp}^{RP} and W_{k}^{K}, which represent the weight of this representative period and the weight of the period k within each rp respectively. Those weights are specified in data sheet Weights. Finally, there is also a mapping $\Gamma(p, rp, k)$ that relates each actual period p to its representative period rp and period k, which is specified in data sheet Hindex.

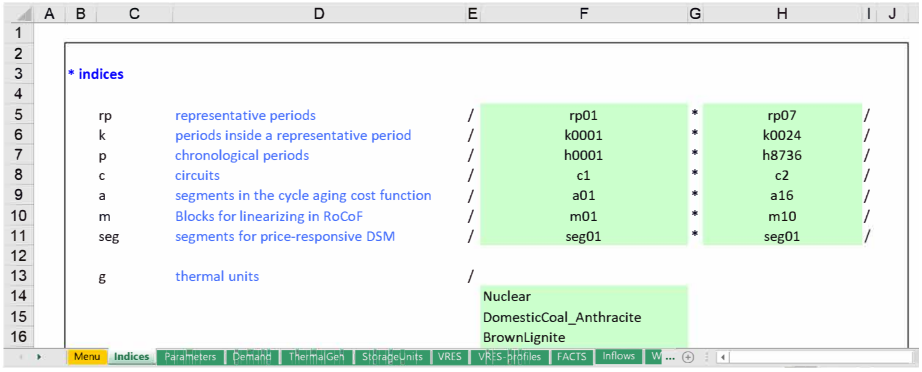

Figure 4: LEGO index and dynamic sets data.

In the example shown in Figure 4, we are representing 8736 chronological hours (p) by using 7 representative periods (rp), each of which has a duration of 24 hours (k). Hence, the corresponding data file uses 7 representative days to capture one year of 8736 chronological hours. If instead, we wanted to run LEGO for the exact hourly model, we would need a data file where index rp is 1 (one representative period which is the entire year). Index k are the chronological periods within the year, so k ranges from 1 to 8736, which would coincide with p in this case. All the weights, both W_{rp}^{RP} and W_k^K, are equal to 1 and $\Gamma(p, rp, k)$ in this case simply associates p with the corresponding k. Note that both data files could correspond to the same original time series of data, e.g., hourly demand data, hourly wind or solar profiles, or hydro inflow data. Given these original time series, one can either use the hourly data directly yielding a LEGO data file corresponding to an exact hourly model, or, one could apply a clustering procedure to the time series and use the clustered data of representative days for example, in a LEGO data file with representative periods.

2.3. Model Outputs

LEGO is a cost minimization optimization model, which - depending on the modules of interest that were chosen - yields a wide variety of outputs (via its primal variables[14]). However, LEGO can also employ dual variables for price information and it can hence be used for economic assessments of particular units or technologies, which makes it a useful tool to study impacts of climate policies on market participants.

How do we use LEGO to obtain price information and to calculate generator profits? If integrality in LEGO is relaxed, then the model becomes a linear program (LP) and dual variables are uniquely defined due to strong duality of LPs. However, in a MIP framework this is not the case. A common practice to obtain prices for MIP models, which has also been adopted in this paper, is to: run the MIP; then fix all integer variables to their optimal value; and

[14] An exhaustive list of these variables is provided in the appendix.

re-run the model as an LP. This method determines equilibrium prices for a given solution. With this in mind, prices are obtained as the dual variables of the corresponding constraints, i.e., the spot market price is the dual variable of the demand balance constraint, reserve market prices are obtained as dual variables of reserve constraints etc.

In that sense, we can calculate profits of each generator and differentiate among different cost and revenue streams as follows:

- Spot market revenues minus spot market purchases (the latter can only occur for storage units). These revenues are calculated using the spot market price, i.e., the dual variable of the demand balance constraint.
- Reserve market revenues minus reserve market O&M cost. Reserve prices are obtained as dual variables of reserve constraints.
- Renewable quota payments. LEGO has a constraint that forces a certain amount of renewable penetration (to mimic policy goals). Its dual can be used to determine corresponding payments.
- Firm capacity payments (should there be any). Firm capacity price is obtained as dual of firm capacity constraint.
- Minus operating costs (variable and fixed).
- Minus investment costs.

3. Mathematical formulation of the LEGO model

In this section we present the mathematical formulation of the LEGO model. However, since LEGO was based on a preliminary model version, presented in [18], in this section we merely focus on the modeling novelties. Constraints that have remained the same are briefly mentioned in the appendix for completeness, but are not addressed here.

The novelties of the model contain: the fact that LEGO does now include demand side management (DSM) discussed in section 3.2; transmission expansion

planning in a DC- and an AC-OPF setting described in section 3.3; a simple representation of the hydrogen sector via an electrolyzer presented in section 3.4.

For the sake of clarity, index g represents all generating units as a whole (both existing and candidate units) in the power sector, and sub-indices t, r, s are thermal, renewable and storage units. On the other hand, index $h2g$ describes hydrogen generating units.

3.1. Objective function and standard constraints

In this section we present the objective function and discuss some other standard constraints. The objective function (1a) represents total system cost as: thermal production cost (start-up cost, commitment cost, and variable cost); potential cost for non-supplied energy; battery degradation cost[15]; cost of providing upward and downward secondary reserve by thermal and storage units; cost of providing demand side management (shifting or shedding demand); generation expansion investment costs for building new units, transmission expansion costs for building new lines, and investment (and O&M) costs of building new hydrogen units; finally, we also consider a potential penalty for hydrogen non-served. Constraint (1b) represents the upper and lower bounds of non-supplied energy; and, (1c) defines investment variables as non-negative integers and establishes an upper bound introduced by parameters $\overline{X}$.

$$
\begin{aligned}
min \sum_{rp,k} W_{rp}^{RP} W_k^K \Big(\sum_t (C_t^{SU} y_{rp,k,t} + C_t^{UP} u_{rp,k,t} + C_t^{VAR} p_{rp,k,t}) \\
+ \sum_r C_r^{OM} p_{rp,k,r} + \sum_s C_s^{OM} p_{rp,k,s} + \sum_i C^{ENS} pns_{rp,k,i} \Big) \\
+ \sum_{rp,k,cdsf(s),a} W_{rp}^{RP} W_k^K C_{s,a}^{CDSF} dis_{rp,k,s,a} \\
+ \sum_{rp,k} W_{rp}^{RP} W_k^K \Big(\sum_t (C_t^{VAR} C^{RES+} res_{rp,k,t}^{+} + C_t^{VAR} C^{RES-} res_{rp,k,t}^{-})
\end{aligned}
$$

[15] If no battery degradation is considered then this term is simply zero.

$$+\sum_{s}(C_s^{OM}C^{RES+}res^{+}_{rp,k,s}+C_s^{OM}C^{RES-}res^{-}_{rp,k,s})\Big)$$

$$+\sum_{rp,k}W_{rp}^{RP}W_k^K\Big(\sum_{i,sec}C^{DSM,-}dsm^{-}_{rp,k,i,sec}+\sum_{i,seg}C^{DSM,S}dsm^{S}_{rp,k,i,seg}\Big)$$

$$+\sum_{g}C_g^{INV}x_g+\sum_{ijcc(i,j,c)}C^{L,Inv}_{i,j,c}x^{L}_{i,j,c}+\sum_{h2g}(C^{H2,INV}_{h2g}+C^{H2,OM}_{h2g})x^{H2}_{h2g}$$

$$+\sum_{rp,k,hi}W_{rp}^{RP}W_k^KC^{HNS}h2ns_{rp,k,hi} \quad (1a)$$

$$0\leq pns_{rp,k,i}\leq D^{P}_{rp,k,i} \quad \forall rp,k,i \quad (1b)$$

$$x_g\in\mathbb{Z}^{+,0}, x_g\leq\overline{X}_g \quad \forall g \quad (1c)$$

Other standard constraints, that have been previously presented in [18] and therefore do not constitute an original contribution of this paper, are briefly mentioned here and listed in the appendix for completeness. For a detailed explanation of these constraints, the reader is referred to [18]. In particular, the constraints regarding thermal power plant operations are given by (7), and the constraints that are specific for storage technologies are given by (8).

Constraints (2) are policy constraints and related to variable renewable energy sources. In particular, (2a) corresponds to lower and upper bounds on renewable production. In order to be able to control renewable penetration, a system-wide constraint that limits thermal production to at most $(1-\kappa)$ percent of total system demand (2b) is also imposed[16], thereby implicitly forcing κ percent clean production. Inspired by [21], we have introduced a firm capacity constraint (2c) where FCC_g is the firm capacity coefficient[17] by technology and FCP is the percentage of firm capacity required by the system (110% here) both have been taken from [21]. In the rMIP framework, the dual of this constraint

[16]Note that if parameter κ is set to zero, this constraint is relaxed

[17]This factor describes the percentage of the installed capacity for each technology that is considered firm. In this context, firm means the capacity available for production or transmission which can be (and in many cases must be) guaranteed to be available at a given time. These coefficients are almost 100% for dispatchable technologies, and usually much lower for intermittent VREs where they could also be a function of the system portfolio.

yields a firm capacity price in €/MW of firm capacity, which is used in firm capacity payments.

$$0 \leq p_{rp,k,r} \leq \overline{P}_r PF_{rp,k,r}(x_r + EU_r) \quad \forall rp, k, r \tag{2a}$$

$$\sum_{rp,k,t} W_k^K W_{rp}^{RP} p_{rp,k,t} \leq (1-\kappa) \sum_{rp,k,i} W_k^K W_{rp}^{RP} D_{rp,k,i}^P \tag{2b}$$

$$\sum_g FCC_g \overline{P}_g (x_g + EU_g) \geq FCP \; D^{peak} \tag{2c}$$

3.2. Demand-side management

One novelty in LEGO is the fact that it can now account for demand-side management (DSM). In particular, we consider two different types of DSM: demand shifting within a given range of hours and demand shedding. In order to do so, we introduce two new indices, i.e., *sec*, which represents the different sectors where DSM shifting is considered (such as electric vehicles, residential heating or residential washing/drying load), and *seg*, which corresponds to the different segments of price-responsive DSM. The DSM shifting that we represent considers that a particular load can be deferred within a particular amount of time. For example, the load of washing and drying at 10am can be deferred for at most 6 hours, so until 4pm but not more. In order to establish the correct relation among inter-day hours where DSM shifting is allowed, we define the dynamic set $dkk_{rp,k,k,sec}$.

In (3) we present the corresponding DSM constraints. Note that DSM also has an impact on the demand balance equations, which are discussed in detail in section 3.3. In order to represent the price-responsive load shedding we have defined variable $dsm^S_{rp,k,i,seg}$, which has an upper bound (3f), appears in the demand balance equation and has a corresponding cost term in the objective function. In order to formulate shifting DSM, we define two variables $dsm^-_{rp,k,i,sec}$ and $dsm^+_{rp,k,i,sec}$ that represent downward shifting and upward shifting of load. A downward shift represents the amount of power that the load is reduced, so in the power balance this variable can be interpreted as reducing demand by that

amount, whereas an upward shift increases demand. In the objective function we consider an explicit cost of a downward shift, which is what the system operator would have to pay a consumer for reducing his/her load. Constraint (3a) defines a balance constraint that ensures that the total upward shifted demand equals the total downward shifted demand over the duration of one representative period. In order to make sure that these shifts are carried within the allowed range of hours, we introduce constraint (3b).

$$\sum_{k} dsm^{+}_{rp,k,i,sec} = \sum_{k} dsm^{-}_{rp,k,i,sec} \quad \forall rp, i, sec \tag{3a}$$

$$dsm^{+}_{rp,k,i,sec} \leq \sum_{kk \in dkk(rp,k,kk,sec)} dsm^{-}_{rp,kk,i,sec} \quad \forall rp, k, i, sec \tag{3b}$$

$$dsm^{+}_{rp,k,i,sec} + dsm^{-}_{rp,k,i,sec} \leq max(\overline{DSM}^{+}, \overline{DSM}^{-}) \quad \forall rp, k, i, sec \tag{3c}$$

$$0 \leq dsm^{-}_{rp,k,i,sec} \leq \overline{DSM}^{-}_{rp,k,i,sec} v^{+/-}_{rp,k,i,sec} \quad \forall rp, k, i, sec \tag{3d}$$

$$0 \leq dsm^{+}_{rp,k,i,sec} \leq \overline{DSM}^{+}_{rp,k,i,sec} (1 - v^{+/-}_{rp,k,i,sec}) \quad \forall rp, k, i, sec \tag{3e}$$

$$0 \leq dsm^{S}_{rp,k,i,seg} \leq \overline{DSM}^{S}_{sec} D^{P}_{rp,k,i} \quad \forall rp, k, i, seg \tag{3f}$$

$$v^{+/-}_{rp,k,i,sec} \in \{0, 1\} \tag{3g}$$

3.3. Transmission expansion planning (DC + AC)

LEGO is flexible and can be solved as a single-node problem, a DC optimal power flow (OPF), and a second-order cone programming (SOCP) approximation of the full AC-OPF. In this paper, we have extended LEGO to include also transmission expansion planning (TEP) of candidate lines. If candidate lines are specified in data sheet Network, see Figure 2, LEGO carries out transmission expansion planning, otherwise it is solved as an OPF. In the remainder of this section we describe the mathematical TEP formulation in DC in section 3.3.1, and in AC in section 3.3.2.

3.3.1. DC-OPF

Constraints (4) represent the optimal power flow in DC and the additional constraints to account for TEP: active power balance constraint (4a), which

contains generation of thermal, renewable and storage technologies, flow to and from the bus, non-supplied energy, and demand side management (shedding and down shifting) and sets it equal to power demand, upward DSM shifting and power consumption of hydrogen units; definition of power flow variable using angle differences for existing (4b) and candidate power lines (4c)-(4d); lower and upper bounds on power flow for existing (4e) and candidate lines (4f); definition of investment variables as binaries by (4g).

$$\begin{aligned}
&\sum_{gi(t,i)} p_{rp,k,t} + \sum_{gi(r,i)} p_{rp,k,r} + \sum_{gi(s,i)} (p_{rp,k,s} - cs_{rp,k,s}) \\
&\qquad + \sum_{ijc(j,i,c)} f^P_{rp,k,j,i,c} - \sum_{ijc(i,j,c)} f^P_{rp,k,i,j,c} \\
&\qquad + pns_{rp,k,i} + \sum_{sec} dsm^-_{rp,k,i,sec} + \sum_{seg} dsm^S_{rp,k,i,seg} \\
&= D^P_{rp,k,i} + \sum_{sec} dsm^+_{rp,k,i,sec} + \sum_{h2gi(h2g,i)} cs^E_{rp,k,h2g} \quad \forall rp,k,i \qquad (4a)
\end{aligned}$$

$$f^P_{rp,k,ijc} = \frac{(\theta_{rp,k,i} - \theta_{rp,k,j})SB}{Reac_{i,j,c}} \quad \forall rp,k,ijce(i,j,c) \qquad (4b)$$

$$f^P_{rp,k,ijc} \leq \frac{(\theta_{rp,k,i} - \theta_{rp,k,j})SB}{Reac_{i,j,c}} + \overline{T}_{i,j,c}(1 - x^L_{i,j,c}) \quad \forall rp,k,ijcc(i,j,c) \qquad (4c)$$

$$f^P_{rp,k,ijc} \geq \frac{(\theta_{rp,k,i} - \theta_{rp,k,j})SB}{Reac_{i,j,c}} - \overline{T}_{i,j,c}(1 - x^L_{i,j,c}) \quad \forall rp,k,ijcc(i,j,c) \qquad (4d)$$

$$-\overline{T}_{i,j,c} \leq f^P_{rp,k,i,j,c} \leq \overline{T}_{i,j,c} \quad \forall rp,k,ijce(i,j,c) \qquad (4e)$$

$$-\overline{T}_{i,j,c} x^L_{i,j,c} \leq f^P_{rp,k,i,j,c} \leq \overline{T}_{i,j,c} x^L_{i,j,c} \quad \forall rp,k,ijcc(i,j,c) \qquad (4f)$$

$$x^L_{i,j,c} \in \{0,1\} \quad \forall ijcc(i,j,c) \qquad (4g)$$

3.3.2. AC-OPF

In this section we present the mathematical formulation of the power flow equations in AC, which have been approximated as a second-order cone program (SOCP) as in [22] and [23].[18] Note that we have introduced candidate lines in

[18]The following auxiliary variables have been used in the SOCP formulation: $cii_{rp,k,i}, cij_{rp,k,i,j}, sij_{rp,k,i,m}$, which represent the square of the voltage at bus i, the product

this formulation in order to carry out TEP in an AC-OPF approximation. In LEGO, in the Parameters sheet, one can specify if a DC-OPF or an SOCP approximation of the AC-OPF should be run. The GAMS code itself then replaces (4) with (5) internally.

Constraints (5) represent: an updated version of: the active power balance equation (5a); a reactive power balance (5b); definition of active power flow from bus i to bus j (5c) and from bus j to bus i (5d) for existing lines[19]; definition of active power flow from bus i to bus j (5e) and from bus j to bus i (5f) for candidate lines; definition of reactive power flow from bus i to bus j (5g) and from bus j to bus i (5h) for existing lines; definition of reactive power flow from bus i to bus j (5i) and from bus j to bus i (5j) for candidate lines; the conic constraint of the SOCP representing the squares of voltages (5k); ensuring maximum angle differences (5l); lower and upper bounds on reactive power provided by FACTS (5m); lower and upper bounds on reactive power provided by thermal units (5n); lower and upper bounds on reactive power provided by unit g (5o)[20]; bounds on active (5p) and reactive (5q) power flow for existing lines; bounds on active (5r) and reactive (5s) power flow for candidate lines; bounds of auxiliary cii variable (5t); bounds of auxiliary cij variable (5u); bounds of auxiliary sij variable (5v).

$$\sum_{gi(t,i)} p_{rp,k,t} + \sum_{gi(r,i)} p_{rp,k,r} + \sum_{gi(s,i)} p_{rp,k,s} - \sum_{gi(s,i)} cs_{rp,k,s} + pns_{rp,k,i}$$

of the voltages at bus i and j times $cos(\theta_{ij})$, and the product of the voltages at bus i and j times $sin(\theta_{ij})$.

[19]In the DC-OPF we do not explicitly consider both directions of the power flow, demonstrated by the fact that equation (4b) is only defined in one direction. This is connected to the underlying DC hypothesis that $f^P_{i,j} = -f^P_{i,j}$, which is not necessarily the case in actual AC power flow. That is why in the SOCP formulation we have to explicitly define and distinguish between the direction of the power flow.

[20]This constraint is redundant for thermal and FACTS given that there are more binding constraints for them available. This is just a general limit to help the numerical solvers, and for storage and renewable units should they be able to provide reactive power.

$$+\sum_{sec} dsm^{-}_{rp,k,i,sec} + \sum_{seg} dsm^{S}_{rp,k,i,seg}$$

$$= \sum_{(j,c)\in ijc(i,j,c)} f^{P}_{rp,k,i,j,c} + \sum_{(j,c)\in ijc(j,i,c)} f^{P}_{rp,k,i,j,c}$$

$$+cii_{rp,k,i}G_i SB + D^{P}_{rp,k,i}$$

$$+\sum_{sec} dsm^{+}_{rp,k,i,sec} + \sum_{h2gi(h2g,i)} cs^{E}_{rp,k,h2g} \quad \forall rp,k,i \tag{5a}$$

$$\sum_{gi(t,i)} q_{rp,k,t} + \sum_{gi(r,i)} q_{rp,k,i} + \sum_{gi(s,i)} q_{rp,k,s} + \sum_{gi(facts,i)} q_{rp,k,facts}$$

$$+pns_{rp,k,i}R_i + \sum_{sec} dsm^{-}_{rp,k,i,sec}R_i + \sum_{seg} dsm^{S}_{rp,k,i,seg}R_i$$

$$= \sum_{(j,c)\in ijc(i,j,c)} f^{Q}_{rp,k,i,j,c} + \sum_{(j,c)\in ijc(j,i,c)} f^{Q}_{rp,k,i,j,c}$$

$$-cii_{rp,k,i}B_i SB + D^{Q}_{rp,k,i}$$

$$+\sum_{sec} dsm^{+}_{rp,k,i,sec}R_i + \sum_{h2gi(h2g,i)} cs^{E}_{rp,k,h2g}R_i \quad \forall rp,k,i \tag{5b}$$

$$f^{P}_{rp,k,i,j,c} = SB[G_{i,j,c}cii_{rp,k,i} - cij_{rp,k,i,j}G_{i,j,c} + sij_{rp,k,i,j}B_{i,j,c}]$$

$$\forall rp,k,ijce(i,j,c) \tag{5c}$$

$$f^{P}_{rp,k,j,i,c} = SB[G_{i,j,c}cii_{rp,k,j} - cij_{rp,k,i,j}G_{i,j,c} - sij_{rp,k,i,j}B_{i,j,c}]$$

$$\forall rp,k,ijce(i,j,c) \tag{5d}$$

$$SB[G_{i,j,c}cii_{rp,k,i} - cij_{rp,k,i,j}G_{i,j,c} + sij_{rp,k,i,j}B_{i,j,c}] - M^{L}(1 - x^{L}_{i,j,c})$$

$$\leq f^{P}_{rp,k,i,j,c} \leq$$

$$SB[G_{i,j,c}cii_{rp,k,i} - cij_{rp,k,i,j}G_{i,j,c} + sij_{rp,k,i,j}B_{i,j,c}] + M^{L}(1 - x^{L}_{i,j,c})$$

$$\forall rp,k,ijcc(i,j,c) \tag{5e}$$

$$SB[G_{i,j,c}cii_{rp,k,j} - cij_{rp,k,i,j}G_{i,j,c} - sij_{rp,k,i,j}B_{i,j,c}] - M^{L}(1 - x^{L}_{i,j,c})$$

$$\leq f^{P}_{rp,k,j,i,c} \leq$$

$$SB[G_{i,j,c}cii_{rp,k,j} - cij_{rp,k,i,j}G_{i,j,c} - sij_{rp,k,i,j}B_{i,j,c}] + M^{L}(1 - x^{L}_{i,j,c})$$

$$\forall rp,k,ijcc(i,j,c) \tag{5f}$$

$$SB[-(B_{i,j,c} + Bc_{i,j,c}/2)cii_{rp,k,i} + sij_{rp,k,i,j}G_{i,j,c} + cij_{rp,k,i,j}B_{i,j,c}]$$

$$= f^{Q}_{rp,k,i,j,c} \quad \forall rp,k,ijce(i,j,c) \tag{5g}$$

$$SB[-(B_{i,j,c} + Bc_{i,j,c}/2)cii_{rp,k,j} - sij_{rp,k,i,j}G_{i,j,c} + cij_{rp,k,i,j}B_{i,j,c}]$$
$$= f^{Q}_{rp,k,j,i,c} \quad \forall rp, k, ijce(i,j,c) \tag{5h}$$

$$SB[-(B_{i,j,c} + Bc_{i,j,c}/2)cii_{rp,k,i} + sij_{rp,k,i,j}G_{i,j,c} + cij_{rp,k,i,j}B_{i,j,c}]$$
$$-M^{L}(1 - x^{L}_{i,j,c}) \leq f^{Q}_{rp,k,i,j,c} \leq M^{L}(1 - x^{L}_{i,j,c}) +$$
$$SB[-(B_{i,j,c} + Bc_{i,j,c}/2)cii_{rp,k,i} + sij_{rp,k,i,j}G_{i,j,c} + cij_{rp,k,i,j}B_{i,j,c}]$$
$$\forall rp, k, ijcc(i,j,c) \tag{5i}$$

$$SB[-(B_{i,j,c} + Bc_{i,j,c}/2)cii_{rp,k,j} - sij_{rp,k,i,j}G_{i,j,c} + cij_{rp,k,i,j}B_{i,j,c}]$$
$$-M^{L}(1 - x^{L}_{i,j,c}) \leq f^{Q}_{rp,k,j,i,c} \leq M^{L}(1 - x^{L}_{i,j,c}) +$$
$$SB[-(B_{i,j,c} + Bc_{i,j,c}/2)cii_{rp,k,j} - sij_{rp,k,i,j}G_{i,j,c} + cij_{rp,k,i,j}B_{i,j,c}]$$
$$\forall rp, k, ijcc(i,j,c) \tag{5j}$$

$$cij^{2}_{rp,k,i,j} + sij^{2}_{rp,k,i,j} \leq cii_{rp,k,i}cii_{rp,k,j} \quad \forall rp, k, line(i,j) \tag{5k}$$

$$-cij_{rp,k,i,j}tan(\Delta) \leq sij_{rp,k,i,j} \leq cij_{rp,k,i,j}tan(\Delta) \quad \forall rp, k, line(i,j) \tag{5l}$$

$$x_{facts}\underline{Q}_{facts} \leq q_{rp,k,facts} \leq x_{facts}\overline{Q}_{facts} \quad \forall rp, k, facts \tag{5m}$$

$$u_{rp,k,t}\underline{Q}_{t} \leq q_{rp,k,t} \leq u_{rp,k,t}\overline{Q}_{t} \quad \forall rp, k, t \tag{5n}$$

$$\underline{Q}_{g} \leq q_{rp,k,g} \leq \overline{Q}_{g} \quad \forall rp, k, g \tag{5o}$$

$$-\overline{T}_{i,j,c} \leq f^{P}_{rp,k,i,j,c} \leq \overline{T}_{i,j,c} \quad \forall rp, k, ijce(i,j,c) \tag{5p}$$

$$-\overline{A}_{i,j,c} \leq f^{Q}_{rp,k,i,j,c} \leq \overline{A}_{i,j,c} \quad \forall rp, k, ijce(i,j,c) \tag{5q}$$

$$-\overline{T}_{i,j,c}x^{L}_{i,j,c} \leq f^{P}_{rp,k,i,j,c} \leq \overline{T}_{i,j,c}x^{L}_{i,j,c} \quad \forall rp, k, ijcc(i,j,c) \tag{5r}$$

$$-\overline{A}_{i,j,c}x^{L}_{i,j,c} \leq f^{Q}_{rp,k,i,j,c} \leq \overline{A}_{i,j,c}x^{L}_{i,j,c} \quad \forall rp, k, ijcc(i,j,c) \tag{5s}$$

$$\underline{V}^{2}_{i} \leq cii_{rp,k,i} \leq \overline{V}^{2}_{i} \quad \forall rp, k, i \tag{5t}$$

$$\underline{V}^{2}_{i} \leq cij_{rp,k,i,j} \leq \overline{V}^{2}_{i} \quad \forall rp, k, line(i,j) \tag{5u}$$

$$-\overline{V}^{2}_{i} \leq sij_{rp,k,i,j} \leq \overline{V}^{2}_{i} \quad \forall rp, k, line(i,j) \tag{5v}$$

3.4. Hydrogen

In LEGO we consider the possibility of producing hydrogen via electrolysis, powered by energy, in order to fulfill an inelastic demand of hydrogen. To that purpose, we define an index $h2g$, which are hydrogen generating units and in this

particular case that would correspond to electrolyzers, each of which consume a particular amount of electric energy $cs^{E}_{rp,k,h2g}$ (MW) in order to produce hydrogen $p^{H2}_{rp,k,h2g}$ (kg), whose bounds are given in (6a). We employ conversion factor HPE_{h2g}, which quantifies how many kg of hydrogen are obtained through electrolysis when using 1 MWh of electric energy, given in (6b). Note that a-priori, hydrogen might flow in a network (i.e., pipelines) different from the transmission grid. Hence, we define index $h2i$, which corresponds to the different nodes of the hydrogen network. However, since an electrolyzer does consume electric energy, it will likely be located at a node $h2i$ that actually coincides bus i of the transmission network. In any case, dynamic set $h2gi(h2g, i)$ determines at what bus the unit $h2g$ is located in order to add the corresponding consumption of electric energy in the power balance equation given in section 3.3. There could be different sectors $h2sec$ in which we have a demand for hydrogen. Constraint (6c) represents the hydrogen balance equation for each sector, which contains the hydrogen production $p^{H2}_{rp,k,h2g}$, and the hydrogen non-served $h2ns_{rp,k,h2i}$ (6d). Constraint (6e) defines discrete investment variables. In future work, we plan to expand the formulation of the hydrogen sector in order to contain a network of pipelines, and other hydrogen-related infrastructure.

$$0 \leq p^{H2}_{rp,k,h2g} \leq \overline{P}^{E}_{h2g} W^{K}_{k} HPE_{h2g} (x^{H2}_{h2g} + EU^{H2}_{h2g}) \quad \forall rp, k, h2g \quad \text{(6a)}$$

$$cs^{E}_{rp,k,h2g} W^{K}_{k} HPE_{h2g} = p^{H2}_{rp,k,h2g} \quad \forall rp, k, h2g \quad \text{(6b)}$$

$$\sum_{h2g h2i(h2g,h2i)} p^{H2}_{rp,k,h2g} + h2ns_{rp,k,h2i} = \sum_{h2sec} D^{H2}_{rp,k,h2i,h2sec} \quad \forall rp, k, h2i \quad \text{(6c)}$$

$$0 \leq h2ns_{rp,k,h2i} \leq \sum_{h2sec} D^{H2}_{rp,k,h2i,h2sec} \quad \forall rp, k, hi \quad \text{(6d)}$$

$$x^{H2}_{h2g} \in \mathbb{Z}^{+,0}, x^{H2}_{h2g} \leq \overline{X}^{H2}_{h2g} \quad \forall h2g \quad \text{(6e)}$$

4. Case Studies

The case studies presented in this section are designed to showcase the modularity and flexibility of LEGO. Section 4.1 compares an exact hourly generation

expansion planning DC-OPF with its corresponding model using only 7 representative days. Section 4.2 considers DSM and section 4.3 assesses hydrogen production, two very promising future technologies that could shift optimal power system planning and operation. Finally, in section 4.4 we carry out a transmission (TEP) and generation (GEP) expansion planning problem that contrasts optimal decision making in an AC framework as opposed to a DC simplification.

4.1. Hourly model versus representative days model

The main objective of this section is to show that the LEGO model supports exact hourly data, as well as approximations of that data via representative days. Instead of having to commit to one inflexible data structure that binds the modeler to a particular time representation, LEGO is capable of handling both, which allows the modeler to decide (or even change ex-post depending on the application).

To that purpose we run an rMIP version[21] of LEGO for the exact hourly data set over the time horizon of an entire year, and for an approximated model using 7 representative days that have been chosen applying k-means to the full time series. Please note that clustered model results depend heavily on the clustering technique; however, it is beyond the scope of this paper to assess the best clustering techniques for expansion planning. We simply picked k-means because it is a standard clustering technique.

Moreover, in this case we do not enforce a particular renewable penetration. However, we do require a 110% firm capacity constraint to be met. The model considers an almost greenfield approach. The only existing technology in the system is hydro. The reason for this is twofold: first, when assessing

[21]The hourly model consists of 8760 individual hours. Running a MIP expansion and UC model for the full hourly model renders models that would exceed the computational infrastructure available to us. Hence, we have decided to run this section as rMIP model for a fair comparison. Note that in other section we do run a MIP version of the representative day model as well.

economic results we wanted to show the difference between existing units and new investments; second, on the transition towards a carbon-neutral future, existing thermal generation assets might be retired, but hydro infrastructure will definitely remain as long as the useful life allows. All other technologies[22] are considered candidate units for investment in a DC-OPF setting. Note that in this case study, there is no transmission expansion.

The values shown in Table 1 represent capacity investment decisions per technology for the representative days case study and the hourly rMIP models. The results show very clearly the importance of accounting for hourly details in generation expansion planning. When considering only 7 representative days, the necessary capacity in peakers, such as OCGTs, is under-estimated (1427 versus 2240 MW). It also seems that when accounting for all individual hours of the year, about 300 MW more CCGT capacity is required. On the other hand, the representative day model version over-estimates the optimal wind capacity by almost 600 MW. The results show to what extent the representative days under-estimate the uncertainty caused by renewable energy sources, which - in reality - would have to be compensated by thermal power plants.

Differences between full hourly and representative days models are to be expected and could be remedied by either increasing the number of representative days, or by choosing representative days more intelligently (than just doing k-means), for example by including extreme-value days.

	CCGT	**OCGT**	**BESS**	**Wind**	**Solar**
7 LRP	2738	1427	210	2202	1269
Hourly	3079	2240	220	1673	1305

Table 1: Capacity investments (MW) per technology in representative days and hourly case studies (firm capacity = 110%)

Table 2 contains the annual production (in GWh) per technology for both temporal representations. In this case study (where no specific renewable pene-

[22] Coal, gas-fired units, solar, wind and batteries.

tration is enforced), the main difference in production between the representative days and the full hourly model are 1000 GWh that are shifted from wind to CCGT production. Note that hydro remains the same in both cases, because the maximum amount of hydro production is limited.

	CCGT	**OCGT**	**BESS**	**Wind**	**Solar**	**Hydro**
7 LRP	22426	130	239	5032	2488	1545
Hourly	23236	216	277	4069	2559	1545

Table 2: Annual production (GWh) per technology in representative days and hourly case studies (firm capacity = 110%)

Finally, in Table 3 we present the economic results obtained through LEGO. Note that LEGO actually yields those results per generating unit, however, for the sake of legibility in Table 3 we have summed them per technology. As discussed in an earlier section, total profits are calculated as: spot market revenues minus spot market purchases (only for BESS), reserve market revenues minus costs, minus O&M costs, minus investment costs, plus RES quota payments (that do not apply here because we are not forcing a particular renewable penetration so they have been omitted in the table), plus firm capacity payments. We can confirm that with a convex model (an rMIP) economic theory is confirmed and new investments fully recover investment costs, as can be seen by the zero profits of all newly built technologies. Hydro was an existing technology and is therefore the only technology that has positive profits in such a model setup.

Table 3 puts in contrast the different economic concepts for the representative days and the full hourly model. This allows us to analyze where the largest deviations between the hourly and the representative days case are. But the profits results in general, are very useful to analyze, for example, in what market a new technology is going to make the most of its money. In the hourly model, the BESS technology makes 1.31 M€ (1.72-0.41) on the reserve market and 8.63 M€ (17.41-8.78) on the spot market. Reserve market profits would be

15% of spot market profits for BESS. For other technologies, this percentage is negligible. These results showcase the contribution of BESS to the reserve market in this case study. We also observe that all technologies obtain firm capacity payments according to the firm capacity installed to make them whole. Note that the model itself determines the firm capacity payment, as the dual variable of the firm capacity constraint. In this case study here, the firm capacity payment amounts to 25.8 k€/MW of firm capacity installed.

	CCGT	OCGT	BESS	Wind	Solar	Hydro
Spot market revenues	1086.44 (1135.70)	9.83 (16.19)	16.12 (17.41)	155.81 (118.88)	106.37 (109.39)	95.06 (94.89)
Spot market costs	0 (0)	0 (0)	-8.32 (-8.78)	0 (0)	0 (0)	0 (0)
Reserve market revenues	0.22 (0.44)	0.67 (0.84)	2.06 (1.72)	0 (0)	0 (0)	0.97 (0.66)
Reserve market costs	-0.22 (-0.44)	-0.26 (-0.35)	-0.49 (-0.41)	0 (0)	0 (0)	0 (0)
O&M costs	-1039.79 (-1083.25)	-10.24 (-16.68)	-0.95 (-1.11)	-10.06 (-8.14)	0 (0)	0 (0)
Investment costs	-114.51 (-128.75)	-35.37 (-55.51)	-13.61 (-14.29)	-159.96 (-121.54)	-107.19 (-110.23)	0 (0)
Firm capacity payments	67.86 (76.30)	35.37 (55.51)	5.19 (5.45)	14.21 (10.80)	0.82 (0.84)	3.87 (3.87)
Total profits	0 (0)	0 (0)	0 (0)	0 (0)	0 (0)	99.90 (99.42)

Table 3: Annual profit (M€) concepts per technology for representative days and the full hourly case (results in parentheses) for a 110% firm capacity requirement.

4.2. Impact of demand-side management

In this section we demonstrate how the impacts of demand-side management (DSM) can affect power system operations. To that purpose we run the MIP version of LEGO for a 100% renewable penetration (not allowing for thermal investments) with and without activating the DSM option associated to constraints (3).

DSM provides the power system with more flexibility, an it is therefore not surprising that the system cost is 3.7% lower with DSM (2432.2 M€) than without (2525.5 M€). Table 4 contains the changes in capacity investments. Batteries are most affected by the incorporation of DSM and suffer a 17.7% decrease in capacity, whereas wind and solar capacity does not change much. Energy production behaves similarly.

	BESS	**Wind**	**Solar**
Investment w/o DSM (GW)	9.6	3.5	18.8
Investment with DSM (GW)	7.9 (-17.7%)	3.4 (-2.9%)	18.6 (-1.1%)
Production w/o DSM (GWh)	11.7	4.4	26.9
Production with DSM (GWh)	10.7 (-8.4%)	4.7 (+5.6%)	26.5 (-1.3%)

Table 4: Investments and production per technology with and without DSM in 100% renewable system. Relative change in parentheses.

In Figure 5 we show the behavior of up- and downward DSM for one representative day at bus 6, which is the highest demand bus. In order to understand DSM patterns, we also look at the spot market price for this day, given in Figure 6, which shows that at midday prices are low and wind is the marginal unit, whereas prices are higher during the remaining hours. Commerce, trade and services (CTS) have a delay time of only one hour and are therefore not used very often. Electric vehicles (EVs) are used more during the day when wind causes low spot prices, and used for down DSM during other hours. Note that in future research we plan to extend the EV DSM formulation to be more specific and to incorporate previously established demand patterns by EV users as we believe this to be more realistic. Cooling and freezing, as well as washing and drying DSM follow a similar pattern.

4.3. Hydrogen production

This version of LEGO also contains the possibility of considering the production of hydrogen via an electrolyzer. We run the rMIP version of LEGO without enforcing renewable penetration and activate the hydrogen option. In

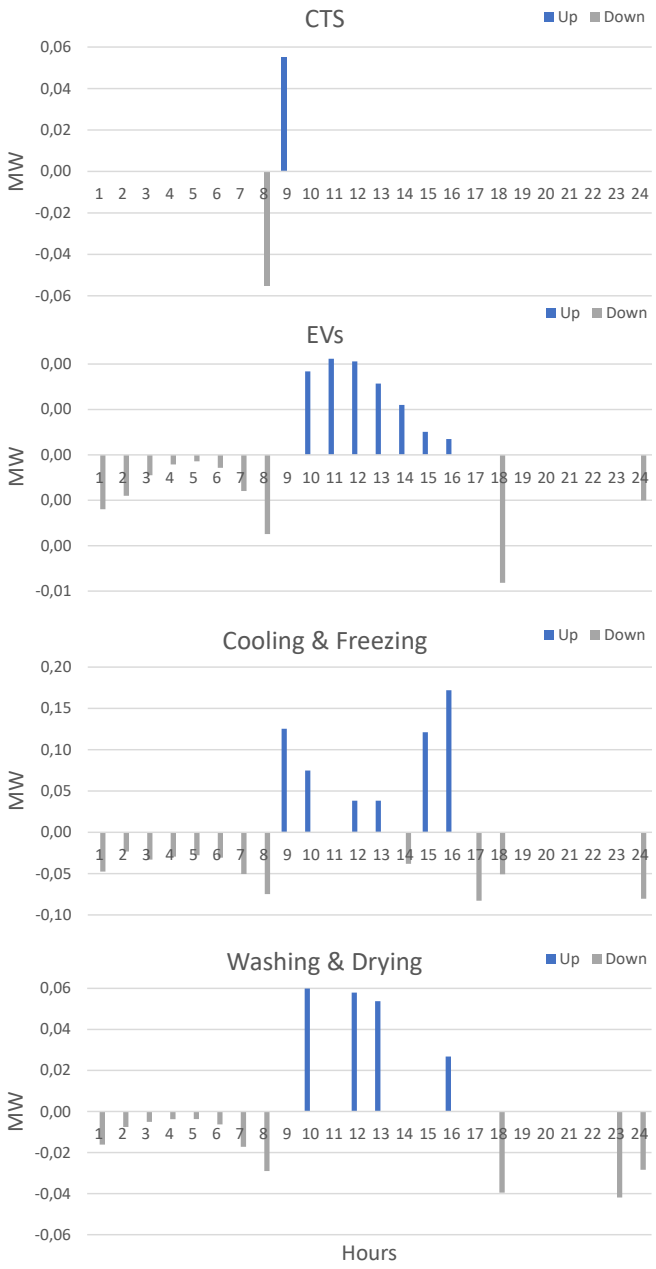

Figure 5: Up and down demand-side management by sector for representative day 4 at bus 6

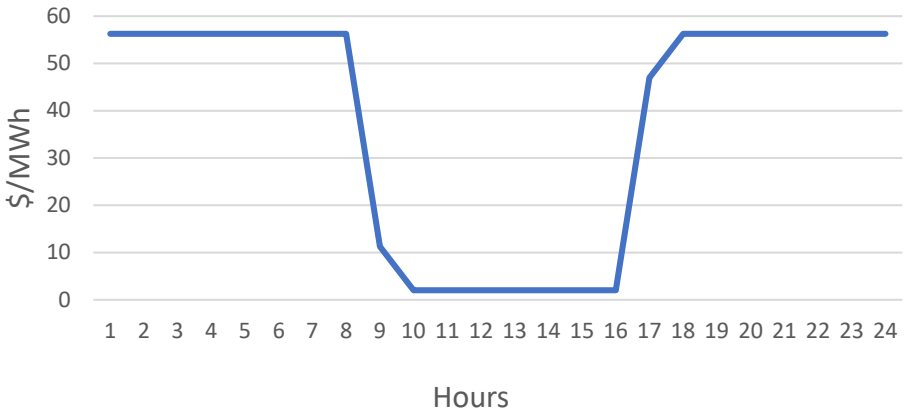

Figure 6: Spot price for representative day 4 at bus 6

this particular case study, we have an annual hydrogen demand of 2190 tonnes that have to be satisfied by one electrolysis plant located at bus 6. We assume that the hydrogen is for industrial use at that bus.

We consider a scenario where energy for the electrolyzer is purchased from the power grid. If we want to determine how clean this hydrogen is, it might be fair to look at the total mix of energy production by technology given in Figure 7, which is 70% CCGTs and 30% clean. The corresponding levelized cost of hydrogen (LCOH) is 2.22 €/kg for this system.

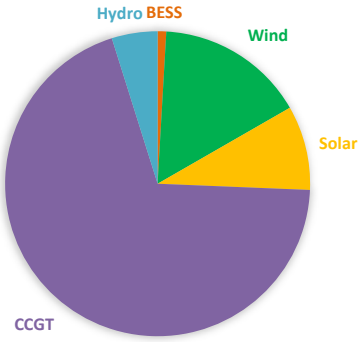

Figure 7: Distribution mix of energy production per technology in power system.

Let us now assume that the industrial demand of hydrogen requires green

hydrogen (and not only 30% green hydrogen). In LEGO, we can add a simple constraint limiting the energy consumption of the electrolyzer by the solar production installed in bus 6. This could be interpreted as locally produced, 100% green hydrogen. Running LEGO with this additional constraint yields a LCOH of 2.4 €/kg. The increase in the LCOH here is caused by the reduced[23] overall hydrogen production due to the limited availability of the intermittent solar resource.

In future research we plan to extend the hydrogen sector to be able to analyze all different types of hydrogen, i.e., green, blue or grey hydrogen.

4.4. Transmission expansion planning DC versus AC

This section shows the results of a MIP version of LEGO, enforcing a 100% renewable penetration and enabling transmission expansion planning under two paradigms: a DC- and an AC-OPF setting. The network is shown in Figure 8.

In this particular data set, the candidate line is built under both DC and AC assumptions (a second circuit between the busses 4 and 5) since building the line allows installing more cheap renewable energy at node 5. And yet, generation investments, power flow, etc., differ significantly. One of the most interesting results is related to the amount of wind capacity installed. Initially, one might be inclined to believe that - since both models build the candidate line between bus 4 and 5 - the newly installed wind capacity at the isolated radial node 5 (where the wind resources are) would also be the same. As shown in Table 5, under the DC-OPF assumption, 7.3 GW of wind capacity is built at bus 5, whereas the AC model only builds 5.8 GW. This result can be explained by analyzing power flow results in more detail. In the DC model, the power flow in line 4-5 is at maximum capacity most of the time. In 3 out of 7 representative days, the line is at maximum capacity for all 24 hours of the day. The flow direction is mostly from bus 5, where the wind is, to the rest of the system via

[23]There is a 12% reduction in total annual hydrogen production for the green hydrogen case.

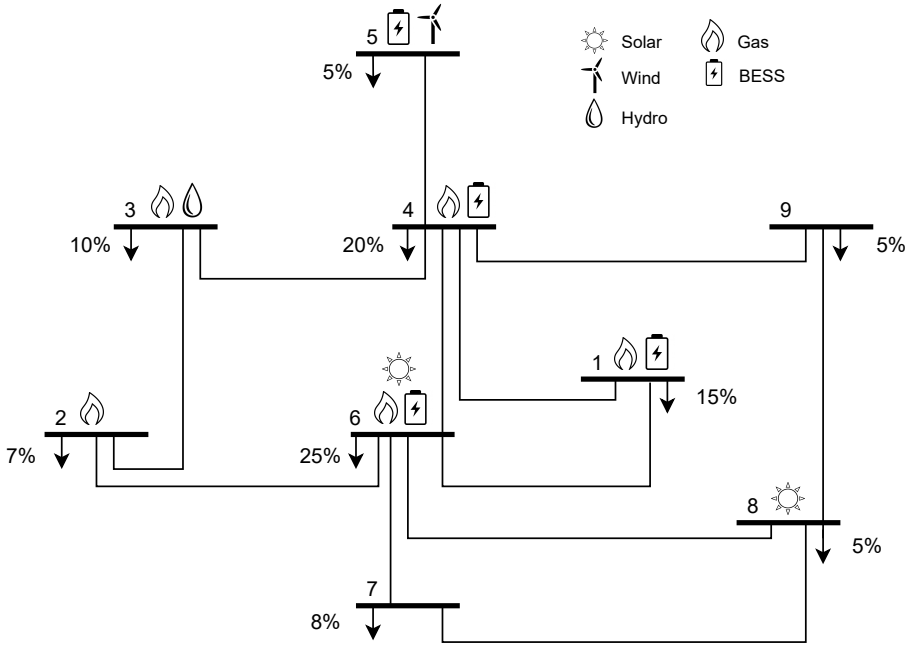

Figure 8: Stylized power system with existing (hydro) and candidate (everything else) generation technologies. Active system demand per bus indicated in percentages.

bus 4.

	BESS	**Wind**	**Solar**	**FACTS**
DC-OPF (GW)	7.6	7.3	12.2	
AC-OPF (GW)	8.0	5.8	15.2	9 **devices**
AC-OPF-tight (GW)	8.3	5.1	16.3	9 **devices**

Table 5: Investments (GW) in 100% renewable system under an AC- and a DC-OPF approach.

However, the DC model does not account for voltage limits nor reactive power. Therefore, when doing so with the AC model, power flow results on this line change drastically. For example, active power flow on line 4-5 never exceeds 85% of line capacity because it also has to account for reactive power flow. Moreover, and more importantly, respecting voltage limits becomes essential here. For instance, transporting large amounts of active power from bus 5 to

bus 4 causes a voltage drop in bus 5. In order to be within the established voltage limits, which we established between 0.9 and 1.1 p.u., voltages in the remaining system (buses 4 etc.) need to be as high as possible but without exceeding limits. These physical limitations cause that the actual active power flow on line 4-5 is, in reality, closer to 85% of maximum capacity (instead of the 100% predicted by the DC-OPF). As a matter of fact, if we tighten the initially established voltage limits to 0.94 and 1.06 p.u. instead, we observe that even less wind capacity can be evacuated via line 4-5 and the distortions concerning the DC-OPF become even more significant.

The total dispatched active power by technology, presented in Table 6, also reflects the differences between the AC and DC. In DC, 9315 GWh of wind production are assumed when in reality, the AC model shows that only 7548 GWh - so 20% less, are cost optimal due to line limitations. For tighter voltage constraints annual wind production would be around 30% less than what is predicted under the DC model. This aggregated result also reflects the impact on the active power flows. Figure 9 shows the detailed active power production per technology for two representative days (number 7 and number 4).

The AC dispatch also considers the reactive power flows through the network, limiting the maximum active power that it is possible to transfer between nodes as explained in the previous paragraph for the particular case in line 4-5.

	BESS	**Wind**	**Solar**	**Hydro**
DC-OPF (GWh)	8837	9315	21689	1545
AC-OPF (GWh)	10096	7548	24121	1545
AC-OPF-tight (GWh)	10561	6683	24990	1545

Table 6: Annual production (GWh) in 100% renewable system under an AC- and a DC-OPF approach.

Another difference between the AC and the DC model is the explicit formulation of provision of reactive power. Especially in a 100% renewable system, a-priori, no generator provides reactive power, which the AC-OPF solves by

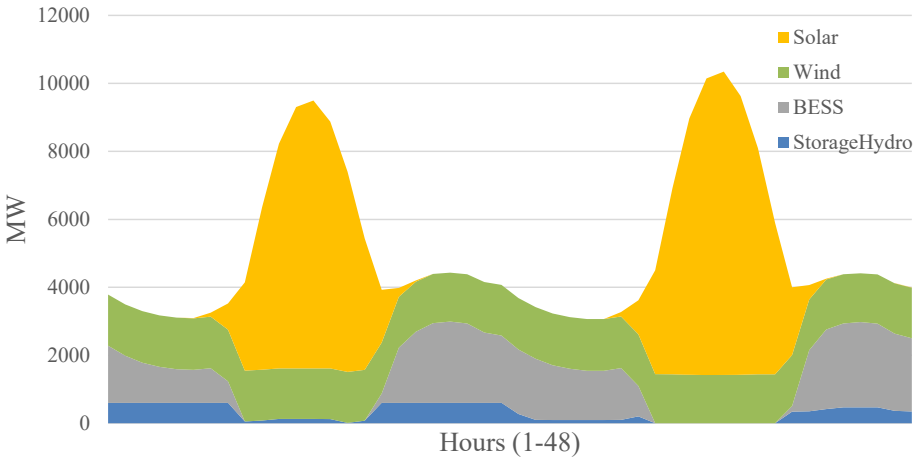

Figure 9: Hourly production (MW) per technology in the 100% renewable system for representative days 7 and 4.

installing 9 FACTs devices. Moreover, the optimal system determined under a DC setting is AC-infeasible due to the lack of provision of reactive power since reactive power is not explicitly accounted for in the DC formulation. When allowing for the ex-post investment of additional FACTS devices, the DC system can be made AC-feasible at an additional system cost of 85 M€. However, such an approach leads to a sub-optimal generation mix.

5. Conclusions

In this paper we presented the full Low-carbon Generation Expansion Optimization (LEGO) model, which is highly flexible and modular. It allows for a multitude of different studies focused on the power sector: short-, medium-, or long-term due to its unique temporal flexible structure; generation planning or operational problems (simply by activating a switch in the data file); transmission expansion planning in either a DC- or an AC-OPF (approximated via SOCP) setting; options to include RoCoF inertia constraints; including demand-side management or the hydrogen sector. To the best of our knowledge there is no single open-source model that combines all of these characteristics. In future

research we plan to extend this model even further by expanding the gas and hydrogen sector, by introducing uncertainty and by introducing a more specific mathematical formulation for electric vehicles.

Acknowledgements

The authors would like to thank the Iberdrola Foundation for funding the REAL project, and J.J. Valentin-Virseda for helpful discussions.

Nomenclature

Acronyms:

AC/DC	Alternating/direct current
BESS	Battery energy storage system
CCGT/OCGT	Combined cycle/Open cycle gas turbine
CTS	Commerce, trade and services
DSM	Demand side management
ESM	Energy system model
EV	Electric vehicle
GEP/TEP	Generation/Transmission expansion planning
LEGO	Low-carbon expansion generation optimization
LP	Linear program
MIP	Mixed integer program
rMIP	Relaxed mixed integer program
MIQCP	Mixed integer quadratically constrained program
OPF	Optimal power flow
O&M	Operations and maintenance
RoCoF	Rate of change of frequency
SOCP	Second-order cone program
UC	Unit commitment

Indices:

p	Time periods (usually hours)
rp	Representative periods (usually days)
k	Time periods within a representative period
$\Gamma(p, rp, k)$	Mapping of periods with representative periods rp and k
g	Generating units
$t(g)$	Subset of thermal generation units
$s(g)$	Subset of storage generation units
$r(g)$	Subset of renewable generation units

$v(g)$	Subset of units that provide virtual inertia
sec	Sectors for demand-side management shifting
seg	Segments for price-responsive DSM
$facts(g)$	Subset of FACTS as reactive power source
i, j, ii	Bus of transmission network
iws	Transmission busses without slack bus
c	Circuit in transmission network
$ijc(i, j, c)$	Transmission line connecting nodes i,j with c
$ijce(i, j, c)$	Existing transmission line connecting nodes i,j with c
$ijcc(i, j, c)$	Candidate transmission line connecting nodes i,j with c
$line(i, j)$	Indicates if a line exists between nodes i and j
$gi(g, i)$	Generator g connected to node i
$h2sec$	Sectors of hydrogen demand
$h2g$	Subset of hydrogen generating units
$h2i, h2j$	Node of hydrogen network
$h2gh2i(h2g, h2i)$	Unit $h2g$ connected to node $h2i$
$h2gi(h2g, i)$	Unit $h2g$ connected to bus i

Parameters:

$D^P_{rp,k,i}$	Active power demand (GW)
$D^Q_{rp,k,i}$	Reactive power demand (GW)
η^{DIS}_g	Discharge efficiency of unit (p.u.)
η^{CH}_g	Charge efficiency of unit (p.u.)
B_i	Susceptance connected at bus i (p.u.)
$B_{i,j,c}$	Line susceptance (p.u.)
$Bc_{i,j,c}$	Branch charging susceptance (p.u.)
G_i	Conductance connected at bus i (p.u.)
$G_{i,j,c}$	Line conductance (p.u.)
SB	Base power (MVA)
R_i	Tan(arccos(pf)) = Q/P at bus i (p.u.)

W_{rp}^{RP}	Weight of the representative period (h)
W_{k}^{K}	Weight of each k within the representative period (h)
C^{ENS}	Cost of energy non-served (M€/GWh)
$C^{DMS,S}$	Cost of DSM shedding (M€/GWh)
$C^{DMS,-}$	Cost of DSM shifing (M€/GWh)
C_{g}^{SU}	Start-up cost of unit (M€)
C_{g}^{UP}	Commitment cost of unit (M€/h)
C_{g}^{VAR}	Variable cost of energy (M€/GWh)
C_{g}^{OM}	Operation and maintenance cost (M€/GWh)
C_{g}^{INV}	Investment cost (M€/GW/y)
$C_{i,j,c}^{L,INV}$	Line investment cost (M€/GW/y)
C^{RES+}	Reserve-up cost (p.u.)
C^{RES-}	Reserve-down cost (p.u.)
RES^{+}	System reserve-up requirement (p.u.)
RES^{-}	System reserve-down requirement (p.u.)
$\underline{P}_{g}$	Technical minimum of unit (GW)
$\overline{P}_{g}$	Technical maximum of unit (GW)
EU_{g}	Indicator of existing unit (integer)
RU_{g}	Ramp-up limit of unit (GW)
RD_{g}	Ramp-down limit of unit (GW)
MOW	Moving window for long-term storage (h)
$PF_{rp,k,i,r}$	Renewable profile per unit and node (p.u.)
$\underline{R}_{s}$	Minimum reserve of storage unit (p.u.)
$M_{rp,k,s}^{ch/d}$	Upper bound on charge and discharge (GW)
$InRes_{s,p}$	Initial reserve (GWh)
$IF_{rp,k,s}$	Inflows (GWh)
κ	Minimum clean (s+r) production (p.u.)
$ISF_{i,j,c,ii}$	Injection Shift Factors (p.u.)
$\overline{T}_{i,j,c}$	Transmission line limit (GW)
$\overline{A}_{i,j,c}$	Apparent power transfer limit (MVA)

Δ	Maximum angle difference (rad)
$\overline{X}_g$	Maximum amount of units to be built (integer)
$\overline{X}^{H2}_{h2g}$	Maximum amount of hydrogen units to be built (integer)
$\overline{X}^{L}_{i,j,c}$	Maximum amount of transmission lines to be built $\in \{0, 1\}$
$D^{H2}_{rp,k,h2i,h2sec}$	Hydrogen demand per sector (t)
HPE_{h2g}	Hydrogen per unit of energy (t/GWh)
$C^{H2,INV}_{h2g}$	Investment cost for hydrogen unit (M€/GW/y)
$\overline{P}^{E}_{h2g}$	Technical maximum of hydrogen unit (GW)
EU^{H2}_{h2g}	Indicator of existing hydrogen units (integer)

Variables:

$p_{rp,k,g}$	Real power generation of the unit (GW)
$\hat{p}_{rp,k,g}$	Real power generation above the technical minimum (GW)
$q_{rp,k,g}$	Reactive power generation of the unit (Gvar)
$cs_{rp,k,g}$	Consumption of the unit (GW)
$pns_{rp,k,i}$	Power non-served (GW)
$f^{P}_{rp,k,i,j,c}$	Real power flow of line ijc (GW)
$f^{Q}_{rp,k,i,j,c}$	Reactive power flow of line ijc (Gvar)
$so^{cii}_{rp,k,i}$	Auxiliary cii variable for SOCP formulation (p.u.)
$y_{rp,k,g}$	Startup decision of the unit (integer)
$z_{rp,k,g}$	Shutdown decision of the unit (integer)
$u_{rp,k,g}$	Dispatch commitment of the unit (integer)
x_g	Investment in generation capacity (integer)
$b^{ch/d}_{rp,k,s}$	Indicator if storage is charging or discharging (binary)
$sp_{rp,k,s}$	Spillages or curtailment (GWh)
$res^{+}_{rp,k,g}$	Secondary reserve up allocation (GW)
$res^{-}_{rp,k,g}$	Secondary reserve down allocation (GW)
$inter_{p,s}$	Inter-period storage reserve or state of charge (GWh)
$p^{H2}_{rp,k,h2g}$	Hydrogen generation of the unit (t)
$cs^{E}_{rp,k,h2g}$	Electric power consumption of the unit (GW)

$h2ns_{rp,k,h2i}$	Hydrogen non-served (t)
x^{H2}_{h2g}	Investment in hydrogen capacity (integer)

Standard Constraints

Note that the constraints described in the appendix here do not constitute an original contribution of this paper, because they have previously been formulated in [18]. However, they are described here for completeness and for facilitating understanding the model for the readers.

Constraints (7) contain all constraints regarding thermal generators: upward reserve requirement (7a); downward reserve requirement (7b); definition of total power output with the technical minimum and output above the technical minimum (7c); limit of upward reserve in case start-up occurred (7d); limit of upward reserve in case shut-down occurs (7e); limit of downward reserve (7f); definition of commitment, start-up and shut-down logic (7g); upper bound of commitment variable (7h); ramp-up constraint (7i); ramp-down constraint (7j); lower and upper bound of total power output (7k); lower and upper bound of reserves and output above the minimum (7l); definition of logical variables as binaries (7m).

With this in mind, we quickly want to define the notation of double minus $--$ or double plus $++$ that appears sometimes in the remainder of this section. The term $k--1$ simply refers to the previous within-time period k. For example, if $k = 2$, then $k--1$ corresponds to $k = 1$. But, if $k = 1$, then $k--1$ corresponds to $k = 24$. The double minus creates a cyclic link between the first and the last k of the same representative period. In the remainder of the paper, we use this terminology for commitment variables and for cyclic storage constraints.

$$\sum_t res^+_{rp,k,t} + \sum_s res^+_{rp,k,s} \geq RES^+ \sum_i D^P_{rp,k,i} \quad \forall rp, k \tag{7a}$$

$$\sum_t res^-_{rp,k,t} + \sum_s res^-_{rp,k,s} \geq RES^- \sum_i D^P_{rp,k,i} \quad \forall rp, k \tag{7b}$$

$$p_{rp,k,t} = u_{rp,k,t}\underline{P}_t + \hat{p}_{rp,k,t} \quad \forall rp, k, t \tag{7c}$$

$$\hat{p}_{rp,k,t} + res^{+}_{rp,k,t} \leq (\overline{P}_t - \underline{P}_t)(u_{rp,k,t} - y_{rp,k,t}) \quad \forall rp, k, t \tag{7d}$$

$$\hat{p}_{rp,k,t} + res^{+}_{rp,k,t} \leq (\overline{P}_t - \underline{P}_t)(u_{rp,k,t} - z_{rp,k++1,t}) \quad \forall rp, k, t \tag{7e}$$

$$\hat{p}_{rp,k,t} \geq res^{-}_{rp,k,t} \quad \forall rp, k, t \tag{7f}$$

$$u_{rp,k,t} - u_{rp,k--1,t} = y_{rp,k,t} - z_{rp,k,t} \quad \forall rp, k, t \tag{7g}$$

$$u_{rp,k,t} \leq x_t + EU_t \quad \forall rp, k, t \tag{7h}$$

$$\hat{p}_{rp,k,t} - \hat{p}_{rp,k--1,t} + res^{+}_{rp,k,t} \leq u_{rp,k,t} RU_t \quad \forall rp, k, t \tag{7i}$$

$$\hat{p}_{rp,k,t} - \hat{p}_{rp,k--1,t} - res^{-}_{rp,k,t} \geq -u_{rp,k--1,t} RD_t \quad \forall rp, k, t \tag{7j}$$

$$0 \leq p_{rp,k,t} \leq \overline{P}_t (x_t + EU_t) \quad \forall rp, k, t \tag{7k}$$

$$0 \leq \hat{p}_{rp,k,t}, res^{-}_{rp,k,t}, res^{+}_{rp,k,t} \leq (\overline{P}_t - \underline{P}_t)(x_t + EU_t) \quad \forall rp, k, t \tag{7l}$$

$$u_{rp,k,t}, y_{rp,k,t}, z_{rp,k,t} \in \{0, 1\} \quad \forall rp, k, t \tag{7m}$$

Constraint (8a) represents the inter-period evolution of the storage state of charge; upper bound of inter storage state of charge (8b); lower bound of inter storage state of charge (8c); cyclic storage constraint (8d); intra-period evolution of storage state of charge (8e); bound of upward reserve (8f); bound of downward reserve (8g); upper bound of intra storage state of charge (8h); lower bound of intra storage state of charge (8i); to avoid simultaneous charging and discharging (8j); definition of binary variable to avoid simultaneous charging and discharging (8k); lower and upper bounds on production, consumption and reserve variables (8l); lower and upper bound of intra storage state of charge (8m); lower and upper bound on spillages (8n).

$$\begin{aligned} inter_{p,s} = inter_{p-MOW,s} + InRes_{s,p=MOW} \\ + \sum_{\Gamma(p-MOW \leq pp \leq p, rp, k)} (-sp_{rp,k,s} + IF_{rp,k,s} W^K_k \\ - p_{rp,k,s} W^K_k / \eta^{DIS}_s + cs_{rp,k,s} W^K_k \eta^{CH}_s) \quad \forall p, s \end{aligned} \tag{8a}$$

$$inter_{p,s} \leq \overline{P}_s ETP_s (x_s + EU_s) \quad \forall s, p : mod(p, MOW) = 0 \tag{8b}$$

$$inter_{p,s} \geq \underline{R}_s \overline{P}_s ETP_s (x_s + EU_s) \quad \forall s, p : mod(p, MOW) = 0 \tag{8c}$$

$$inter_{p,s} \geq InRes_{s,p} \quad \forall s, p = CARD(p) \tag{8d}$$

$$intra_{rp,k,s} = intra_{rp,k--1,s} - sp_{rp,k,s} + IF_{rp,k,s}W_k^K$$

$$-p_{rp,k,s}W_k^K/\eta_s^{DIS} + cs_{rp,k,s}W_k^K\eta_s^{CH}) \quad \forall rp,k \tag{8e}$$

$$\hat{p}_{rp,k,s} - cs_{rp,k,s} + res^+_{rp,k,s} \leq \overline{P}_s(bx_s + EU_s) \quad \forall rp,k,s \tag{8f}$$

$$\hat{p}_{rp,k,s} - cs_{rp,k,s} - res^-_{rp,k,s} \geq -\overline{P}_s(bx_s + EU_s) \quad \forall rp,k,s \tag{8g}$$

$$intra_{rp,k,s} \leq \overline{P}_s ETP_s(x_s + EU_s)$$

$$-(res^-_{rp,k,s} + res^-_{rp,k--1,s})W_k^K \quad \forall rp,k,s \tag{8h}$$

$$intra_{rp,k,s} \geq \underline{R}_s\overline{P}_s ETP_s(x_s + EU_s)$$

$$+(res^+_{rp,k,s} + res^+_{rp,k--1,s})W_k^K \quad \forall rp,k,s \tag{8i}$$

$$p_{rp,k,s} \leq b^{ch/d}_{rp,k,s}M^{ch/d}, cs_{rp,k,s} \leq (1 - b^{ch/d}_{rp,k,s})M^{ch/d} \quad \forall rp,k,s \tag{8j}$$

$$b^{ch/d}_{rp,k,s} \in \{0,1\} \quad \forall rp,k,s \tag{8k}$$

$$0 \leq p_{rp,k,s}, cs_{rp,k,s}res^-_{rp,k,s}, res^+_{rp,k,s} \leq \overline{P}_s(bx_s + EU_s) \quad \forall rp,k,s \tag{8l}$$

$$ETP_s\overline{P}_s\underline{R}_s(x_s + EU_s) \leq intra_{rp,k,s} \leq ETP_s\overline{P}_s(x_s + EU_s) \quad \forall rp,k,s \tag{8m}$$

$$0 \leq sp_{rp,k,s} \leq (1 - \overline{R}_s)ETP_s\overline{P}_s(x_s + EU_s) \quad \forall rp,k,s = hydro \tag{8n}$$

Battery degradation

The constraints in (8) do not account for battery degradation and the corresponding arising costs. According to [], battery degradation has a significant impact on both battery operation and investment decisions. Therefore, we have decided to include the option of considering battery degradation in our model, following the methodology proposed by [**?**] that approximates the rainflow algorithm, as follows in (9). To that purpose we introduce the additional index a that represents the segments of the cycle aging cost function. If battery degradation is considered, then constraints (9) are included in the modeling process, and (8e) is no longer written for storage technologies s that represent batteries.

$$p_{rp,k,s} = \sum_a dis_{rp,k,s,a} \quad \forall rp,k,cdsf(s) \tag{9a}$$

$$cs_{rp,k,s} = \sum_a ch_{rp,k,s,a} \quad \forall rp,k,cdsf(s) \tag{9b}$$

$$intra_{rp,k,s} = \sum_{a} soc_{rp,k,s,a} \quad \forall rp, k, cdsf(s) \tag{9c}$$

$$0 \leq soc_{rp,k,s,a} \leq \overline{P}_s(x_s + EU_s)ETP_s/CARD(a) \quad \forall rp, k, cdsf(s), a \tag{9d}$$

$$soc_{rp,k,s,a} = soc_{rp,k--1,s,a} - dis_{rp,k,s,a}W_k^k/\eta_s^{DIS} + ch_{rp,k,s,a}W_k^k\eta_s^{CH} \quad \forall rp, k, cdsf(s) \tag{9e}$$

Modeling Inertia

Let us now describe in detail the corresponding inertia constraints (10) for a generation expansion framework: definition of the scaled power gain factor of a thermal unit (10a), which represents how much one particular (dispatched) thermal unit can contribute with respect to the total dispatched thermal capacity in the system; definition of the scaled power gain factor of a virtual unit (such as a wind turbine or a battery) (10b), which is defined slightly differently from the corresponding factor of a synchronous generator because it does not have a commitment variable. It is therefore defined as the fraction of its current power output over the total available virtual power output in this moment[24]. Definition of inertia provided by synchronous generators (10c) and virtual generators (10d). The right-hand side of (10d) is multiplied by x_v because $k_{rp,k,v}$ represents the power gain factor for one unit of the virtual technology v. However, in total x_v total units of technology v are built. In (10c) this number is guaranteed to be 1, and that is why it is not explicitly modeled in (10c). Definition of total system inertia (10e): note that total system inertia is a weighted average of virtual inertia and synchronous generator inertia. Rate of change of frequency (RoCoF) constraint (10f). Lower and upper bounds on inertia variables (10g). Lower and upper bounds on power gain factors (10h). The nonlinear constraints in (10), and in particular constraints (10a), (10b), (10d), and (10e), are linearized as described in [18].

[24] In a system where there is a large amount of wind curtailment, this would be an overly conservative approximation.

$$k_{rp,k,t} = \frac{\overline{P}_t}{\sum_{tt} \overline{P}_{tt} u_{rp,k,tt}} u_{rp,k,t} \quad \forall rp, k, t \quad (10a)$$

$$k_{rp,k,v} = \frac{p_{rp,k,t}}{\sum_{vv} \overline{P}_{vv}(x_{vv} + EU_{vv}) PF_{rp,k,vv}} \quad \forall rp, k, v \quad (10b)$$

$$M^{SG}_{rp,k} = \sum_t 2k_{rp,k,t} H_t \quad \forall rp, k \quad (10c)$$

$$M^{VI}_{rp,k} = \sum_v 2k_{rp,k,v} H_v x_v \quad \forall rp, k \quad (10d)$$

$$M_{rp,k} = \frac{M^{SG}_{rp,k} \sum_{tt} \overline{P}_{tt} u_{rp,k,tt} + M^{VI}_{rp,k} \sum_{vv} \overline{P}_{vv}(x_{vv} + EU_{vv}) PF_{rp,k,vv}}{\sum_{tt} \overline{P}_{tt} u_{rp,k,tt} + \sum_{vv} \overline{P}_{vv}(x_{vv} + EU_{vv}) PF_{rp,k,vv}}$$

$$\forall rp, k \quad (10e)$$

$$\frac{\dot{f}_{lim}}{f_b} M_{rp,k} \geq \Delta P_{rp,k} \quad \forall rp, k \quad (10f)$$

$$0 \leq M^{VI}_{rp,k}, M^{SG}_{rp,k}, M_{rp,k} \leq \overline{M} \quad \forall rp, k \quad (10g)$$

$$0 \leq k_{rp,k,g} \leq 1 \quad \forall rp, k, g \quad (10h)$$

References

[1] The Biden plan to build a modern, sustainable infrastructure and an equitable clean energy future, `https://joebiden.com/clean-energy/`.

[2] The European Commission, Communication of the commission. A clean planet for all, The European Commission, 2018.

[3] S. C. Bhattacharyya, G. R. Timilsina, A review of energy system models, International Journal of Energy Sector Management.

[4] General algebraic modeling system (GAMS), https://www.gams.com/.

[5] J. D. Jenkins, N. A. Sepulveda, Enhanced decision support for a changing electricity landscape: the genx configurable electricity resource capacity expansion model.

[6] D. A. Tejada-Arango, M. Domeshek, S. Wogrin, E. Centeno, Enhanced representative days and system states modeling for energy storage investment analysis, IEEE Transactions on Power Systems 33 (6) (2018) 6534–6544.

[7] S. Gonzato, K. Bruninx, E. Delarue, Long term storage in generation expansion planning models with a reduced temporal scope, Applied Energy 298 (2021) 117168.

[8] L. Hirth, The european electricity market model emma, Neon Neue Energieökonomik GmbH, Tech. Rep. Version (2017) 07–12.

[9] A. Ramos, opentepes mathematical formulation, https://opentepes.readthedocs.io/en/latest/MathematicalFormulation.html.

[10] M. Doquet, R. Gonzalez, S. Lepy, E. Momot, F. Verrier, A new tool for adequacy reporting of electric systems: Antares, CIGRE 2008 session, paper C1-305, Paris.

[11] J. Aghaei, M.-I. Alizadeh, Demand response in smart electricity grids equipped with renewable energy sources: A review, Renewable and Sustainable Energy Reviews 18 (2013) 64–72.

[12] G. Strbac, Demand side management: Benefits and challenges, Energy policy 36 (12) (2008) 4419–4426.

[13] L. Göransson, J. Goop, T. Unger, M. Odenberger, F. Johnsson, Linkages between demand-side management and congestion in the european electricity transmission system, Energy 69 (2014) 860–872.

[14] A. Zerrahn, W.-P. Schill, On the representation of demand-side management in power system models, Energy 84 (2015) 840–845.

[15] J. Haas, F. Cebulla, W. Nowak, C. Rahmann, R. Palma-Behnke, A multi-service approach for planning the optimal mix of energy storage technologies in a fully-renewable power supply, Energy Convers. Manag. 178 (2018) 355–368. doi:10.1016/j.enconman.2018.09.087.

[16] X. Zhang, K. W. Chan, H. Wang, J. Hu, B. Zhou, Y. Zhang, J. Qiu, Game-theoretic planning for integrated energy system with independent participants considering ancillary services of power-to-gas stations, Energy 176 (2019) 249–264. doi:10.1016/j.energy.2019.03.154.

[17] Y. Tao, J. Qiu, S. Lai, J. Zhao, Y. Xue, Carbon-Oriented Electricity Network Planning and Transformation, IEEE Trans. Power Syst. 36 (2) (2021) 1034–1048. doi:10.1109/TPWRS.2020.3016668.

[18] S. Wogrin, D. Tejada-Arango, S. Delikaraoglou, A. Botterud, Assessing the impact of inertia and reactive power constraints in generation expansion planning, Applied Energy 280 (2020) 115925.

[19] L. Reichenberg, A. S. Siddiqui, S. Wogrin, Policy implications of downscaling the time dimension in power system planning models to represent variability in renewable output, Energy 159 (2018) 870–877.

[20] S. Wogrin, E. Centeno, J. Barquin, Generation capacity expansion in liberalized electricity markets: A stochastic mpec approach, IEEE Transactions on Power Systems 26 (4) (2011) 2526–2532.

[21] T. Gerres, J. P. C. Ávila, F. M. Martínez, M. R. Abbad, R. C. Arín, Á. S. Miralles, Rethinking the electricity market design: Remuneration mechanisms to reach high res shares. results from a spanish case study, Energy Policy 129 (2019) 1320–1330.

[22] S. H. Low, Convex relaxation of optimal power flow—part i: Formulations and equivalence, IEEE Transactions on Control of Network Systems 1 (1) (2014) 15–27.

[23] S. H. Low, Convex relaxation of optimal power flow—part ii: Exactness, IEEE Transactions on Control of Network Systems 1 (2) (2014) 177–189.